Explicit approximations to estimate the perturbative diffusivity in the presence of convectivity and damping. III. Cylindrical approximations for heat waves traveling inwards

Explicit approximations to estimate the perturbative diffusivity in the presence of convectivity and damping (Part 3): cylindrical approximations for heat waves traveling inwards

M. van Berkel[1,2,3], N. Tamura[1], G.M.D. Hogeweij[2], H. J. Zwart[3], S. Inagaki[4], M.R. de Baar[2,3], and K. Ida[1]

[1]*National Institute for Fusion Science, 322 Oroshi-cho, Toki-city, Gifu, 509-5292, Japan*

[2]*FOM Institute DIFFER-Dutch Institute for Fundamental Energy Research, Association EURATOM- FOM, Trilateral Euregio Cluster, PO Box 1207, 3430 BE Nieuwegein, The Netherlands*

[3]*Eindhoven University of Technology, Dept. of Mechanical Engineering, Control Systems Technology group, PO Box 513, 5600 MB Eindhoven, The Netherlands and*

[4]*Research Institute for Applied Mechanics, Kyushu University, Kasuga 816-8580, Japan*

Abstract

In this paper, a number of new explicit approximations are introduced to estimate the perturbative diffusivity (χ), convectivity (V), and damping (τ) in cylindrical geometry. For this purpose the harmonic components of heat waves induced by localized deposition of modulated power are used. The approximations are based on the heat equation in cylindrical geometry using the symmetry (Neumann) boundary condition at the plasma center. This means that the approximations derived here should be used only to estimate transport coefficients between the plasma center and the off-axis perturbative source. If the effect of cylindrical geometry is small, it is also possible to use semi-infinite domain approximations presented in Part 1 and Part 2 of this series.

A number of new approximations are derived in this part based on continued fractions of the modified Bessel function of the first kind and the Confluent Hypergeometric Function of the first kind. These approximations together with the approximations based on semi-infinite domains are compared here for heat waves traveling towards the center. The relative error for the different derived approximations is presented for different values of frequency, transport coefficients, and dimensionless radius. Moreover, it is shown how combinations of different explicit formulas can be combined to estimate the transport coefficients over a large parameter range for cases without convection and damping, cases with damping only, and cases with convection and damping. The relative error between the approximation and its underlying model is below 2% for the case only diffusivity and damping is considered. If also convectivity is considered, the diffusivity can be estimated well in a large region, but there is also a large region in which no suitable approximation is found.

This paper is the third part (Part 3) of a series of three papers. In Part 1 the semi-infinite slab approximations have been treated. In Part 2 cylindrical approximations are treated for heat waves traveling towards the plasma edge assuming a semi-infinite domain.

I. INTRODUCTION

This paper, Part 3 of a series of three papers, deals with cylindrical approximations based on a symmetry (Neumann) boundary condition that can be used to calculate the perturbative diffusivity χ, convectivity V, and damping τ from the experimental data of heat pulse propagation. These approximations should be used in the case heat waves travel towards the center of the plasma, which is the case when the plasma is perturbated using an off-axis heating source. For a general introduction of the series of three papers the reader is referred to [1].

This paper is structured as follows. Section II gives an overview of the relevant assumptions and models used for perturbative transport analysis. Then, in Section III continued fractions are used to find approximations for χ, V, and τ. Section IV gives an overview and comparison of possible explicit approximations that can be used to estimate χ, V, and τ for heat waves traveling towards the center. In Section V the main results are summarized and discussed for Part C and in Section VI a general conclusion for the set of papers is given.

II. MODELING OF THERMAL TRANSPORT

This section shortly reviews the relevant Partial Differential Equation describing transport in fusion reactors and its solution based on common assumptions in the Laplace domain. This solution is necessary to derive explicit approximations for the transport coefficients, which is the subject of the next section. For a more extensive discussion on the heat equation the reader is referred to [1, 2].

A. Perturbative transport analysis

Linearized thermal transport inside a fusion reactor is often modeled as an one-dimensional radial transport in cylindrical geometry due to the magnetic confined plasma topology [1, 3, 4]

$$\begin{aligned}\frac{3}{2}\frac{\partial}{\partial t}\left(nT\right) = \frac{1}{\rho}\frac{\partial}{\partial \rho}\left(n\rho\chi\left(\rho\right)\frac{\partial T}{\partial \rho} + n\rho V\left(\rho\right)T\right) \\ - \frac{3}{2}n\tau_{inv}\left(\rho\right)T + P_{mod},\end{aligned} \tag{1}$$

where χ is the diffusivity, V the convectivity, τ_{inv} is the damping ($\tau_{inv} = 1/\tau$), T denotes the electron temperature, n the density, ρ the radius, and P_{mod} a perturbative heat source. Analytical models based on (1) can be derived using a number of common assumptions. These assumptions are [2, 3, 5]: constant transport coefficients with respect to time and ρ (homogenous or uniform); no transients due to initial conditions; on the considered domains $P_{mod} = 0$; and density n is assumed constant with respect to ρ and time.

Under these assumptions the analytical solution of (1) in the Laplace domain can be expressed in terms of Confluent Hypergeometric Functions Φ and Ψ [2, 6–8]:

$$\Theta(\rho, s) = e^{\lambda_1 \rho} D_1(s)\, \Psi\left(\frac{\lambda_2}{\lambda_2 - \lambda_1}, 1, (\lambda_2 - \lambda_1)\,\rho\right) + e^{\lambda_1 \rho} D_2(s)\, \Phi\left(\frac{\lambda_2}{\lambda_2 - \lambda_1}, 1, (\lambda_2 - \lambda_1)\,\rho\right), \tag{2}$$

where

$$\lambda_{1,2} = -\frac{V}{2\chi} \mp \sqrt{\left(\frac{V}{2\chi}\right)^2 + \frac{3}{2}\frac{s + \tau_{inv}}{\chi}}, \tag{3}$$

with boundary constants $D_1(s)$ and $D_2(s)$ and the Laplace transformed temperature $\Theta = \mathcal{L}(T)$ where the Laplace variable $s = i\omega$. If $V = 0$, (2) can be simplified in terms of modified Bessel functions I_ν and K_ν of order $\nu = 0$ resulting in [6, 9]

$$\Theta(\rho, s) = \frac{1}{\sqrt{\pi}} D_1(s)\, K_0(z\rho) + D_2(s)\, I_0(z\rho), \tag{4}$$

with

$$z = \sqrt{\frac{3}{2}\frac{s + \tau_{inv}}{\chi}}. \tag{5}$$

The unknown boundary constants $D_1(s)$ and $D_2(s)$ need to be determined or partly eliminated such that analytical models can be determined, which are used in the next section to calculate χ explicitly.

B. Logarithmic temperature derivative and transfer function

In [1, 2] models have been derived to determine χ for heat waves traveling outwards in a cylindrical semi-infinite domain. The semi-infinite domain is in principle unnatural as there is a true other boundary (in the form of a plasma end or wall). However, this assumption is necessary to find approximations for χ, V, and τ_{inv}. On the other hand, if heat waves travel

towards the center in a cylindrical geometry the natural boundary condition is a symmetry (Neumann) boundary condition at $\rho = 0$, i.e.

$$\frac{\partial \Theta(\rho = 0)}{\partial \rho} = 0. \tag{6}$$

In case $V = 0$ for this boundary condition then $D_1(s) = 0$ in (4), which is shown in [10]. This implies that also $D_1(s) = 0$ in (2) when $V \neq 0$. However, this is difficult to prove analytically. Instead, it is numerically verified that $D_1(s) = 0$ in (2) by comparing it to finite difference simulations with boundary condition $\partial T(\rho = 0)/\partial \rho = 0$. This shows that the error between the analytic and numerical simulations are small and that the error is decreasing with increasing density of the discretization grid. Hence, it is concluded that $D_1(s) = 0$ for a Neumann boundary condition in (2), i.e.

$$\Theta(\rho, s) = D_2(s)\, e^{\lambda_1 \rho} \Phi\left(\frac{\lambda_2}{\lambda_2 - \lambda_1}, 1, (\lambda_2 - \lambda_1)\rho\right). \tag{7}$$

Basically, there are two possibilities to handle the unknown $D_2(s)$. One possibility is to use the logarithmic temperature derivative $(\partial\Theta/\partial\rho)/\Theta$ to eliminate $D_2(s)$, where $\Theta = A\exp(i\phi)$ resulting in

$$\frac{\Theta'}{\Theta} = \lambda_1 + \lambda_2 \frac{\Phi(a+1, 2, (\lambda_2 - \lambda_1)\rho)}{\Phi(a, 1, (\lambda_2 - \lambda_1)\rho)}, \tag{8}$$

with the left hand side

$$\frac{\Theta'}{\Theta} = \frac{A'}{A} + i\phi'. \tag{9}$$

Note, that the derivatives are defined in terms of ρ and not in terms of distance to the source. Hence, the derivatives are defined positively for heat waves traveling towards the center. If $V = 0$, this simplifies to

$$\frac{\Theta'}{\Theta} = z \frac{I_1(z\rho)}{I_0(z\rho)} \tag{10}$$

where z is defined according to (5). This last relationship is well known in the literature [5, 10]. In the logarithmic temperature derivative representation it is however necessary to approximate spatial derivatives A'/A and ϕ' from the measured A and ϕ. This can also be avoided using the transfer function representation where $D_2(s)$ is fixed by assuming a second boundary condition.

The most logical choice for a second boundary condition is $\Theta(\rho, s) = \Theta(\rho_1, s)$, which is a weak assumption as $\Theta(\rho_1, s)$ is measured. The transfer function using (7) then becomes

$$\frac{\Theta(\rho_2, s)}{\Theta(\rho_1, s)} = e^{\lambda_1 \Delta\rho} \frac{\Phi(a, 1, (\lambda_2 - \lambda_1)\rho_2)}{\Phi(a, 1, (\lambda_2 - \lambda_1)\rho_1)}, \tag{11}$$

where the solution at a second measurement point $\rho_1 > \rho_2$ is used as resulting temperature $\Theta(\rho_2)$. This description is expressed directly in terms of the measured Fourier coefficients ($\Theta = A\exp(i\phi)$). However, it is not straightforward to derive explicit relationships for χ, V, and τ_{inv} using this relationship.

III. DERIVATION OF EXPLICIT APPROXIMATIONS

In this section, continued fractions are used to find approximations for the transport coefficients in cylindrical geometry using (8) and (10). In the previous section, the logarithmic temperature derivative is introduced, which is described by the ratio of modified Bessel functions of the first kind or Confluent Hypergeometric Functions of the first kind. It is well known in the literature that these ratio's of transcendental functions can be approximated by truncation of their continued fraction representation [2, 11, 12]. Based on this concept a number of new approximations are derived, which are summarized in Tables in the next section and their derivations can be found in the appendix. Here, only the three most important approximations are introduced.

A. Diffusivity and damping only

The continued fraction for a ratio of Bessel functions of the first kind is used to find approximations for χ under influence of damping ($V = 0$). Therefore, the logarithmic temperature derivative introduced in (10) is used. The following continued S-fraction of the ratio of Bessel functions can be found in [12](p. 362)

$$\frac{I_1(z\rho)}{I_0(z\rho)} = \cfrac{a_1}{1+\cfrac{a_2}{1+\frac{a_3}{1+\ldots}}}, \tag{12}$$

where $a_{k+1} = (z\rho)^2/(4k(k+1))$ and $a_1 = z\rho/2$. If this continued fraction is truncated taking only the first term a_1 into account, the logarithmic temperature derivative in (10) is approximated by

$$\frac{\Theta'}{\Theta} = z\frac{z\rho}{2}. \tag{13}$$

This can be solved in terms of χ and τ_{inv} using (5) resulting in

$$\chi_{Is\phi} = \frac{3}{4}\frac{\omega}{\phi'}\rho \qquad \text{and} \qquad \tau_{Is\phi} = \frac{\omega}{\phi'}\frac{A'}{A}. \tag{14}$$

This relationship can also be found based on the asymptotic expansions given in [13].

This method can also be used to find more accurate approximations by using more terms in the continued fraction before truncation. In this case the best approximation is found by truncating at a_4 in (12), which can be written in terms of a third order polynomial in z^2

$$0 = c_2 z^4 + c_1 z^2 + c_0, \tag{15}$$

with coefficients

$$c_2 = 12\rho^3 - \frac{\Theta'}{\Theta}\rho^4,\ c_1 = 192\rho - 72\frac{\Theta'}{\Theta}\rho^2, \text{ and } c_0 = -384\frac{\Theta'}{\Theta}, \tag{16}$$

where Θ'/Θ is given by (9). The third order polynomial yields three solutions in terms of z^2. However, generally only one solution can be used to determine χ, because z^2 is bounded in the first quadrant of the complex plane ($\chi > 0$, $\tau_{inv} > 0$) and the other two are often outside this domain. However, using a truncation of (12) at location a_5 results in more solutions within this domain. Hence, it is no longer straightforward to select the correct solution. This is impractical and as will be shown later unnecessary. Therefore, truncations higher than a_4 will not be considered here. For the truncation using a_4 as the last term, it has been numerically determined that the correct zero is given by

$$z^2 = \frac{-c_1 + \sqrt{c_1^2 - 4\,c_0\,c_2}}{c_2}, \tag{17}$$

which covers the largest region of interest. The solution for the diffusivity χ and the damping τ_{inv} is found by substituting (17) into

$$\chi = \frac{3}{2}\frac{\omega}{\Im\left(z^2\right)} \tag{18}$$

and

$$\tau_{inv} = \omega\frac{\Re\left(z^2\right)}{\Im\left(z^2\right)}. \tag{19}$$

The continued fraction in (12) can also be used to find two other approximations belonging to a_2 and a_3, which are named χ_{Is2} and χ_{Is3}, respectively. These can found in Table II in the next section. In the appendix another continued fraction for the ration of Bessel functions

of the first kind is presented, which is also used to find explicit approximations for χ and τ_{inv}.

In this subsection, the convectivity is assumed zero such that the continued fractions for Bessel functions can be considered. In the next subsection also V is considered, which requires the continued fraction for the ratio of Confluent Hypergeometric Functions of the fist kind to be used to find approximations for χ.

B. Diffusivity, convectivity, and damping

The logarithmic amplitude derivative A'/A and phase derivative ϕ' are given in (8) as function of χ, V, and τ_{inv}. However, only two quantities are known, i.e. A'/A and ϕ', whereas on the right hand side three unknowns are given. Therefore, a third quantity needs to be introduced to calculate the transport coefficients, which can be done by introducing a second harmonic, i.e. $A'(\omega_2)/A(\omega_2)$ or $\phi'(\omega_2)$. In addition, (8) needs to be approximated using a continued fraction. In this case the continued C-fraction of the ratio of Confluent Hypergeometric Functions of the first kind is used

$$\frac{\Phi(a+1,b+1,z)}{\Phi(a,b,z)} = \cfrac{1}{1-\cfrac{\frac{b-a}{(b+0)(b+1)}z}{1+\left.\cfrac{\frac{a+1}{(b+1)(b+2)}z}{1-\cfrac{\frac{b-a+1}{(b+2)(b+3)}z}{1+\left.\cfrac{\frac{a+2}{(b+3)(b+4)}z}{1-\ddots}\right|_b}}\right|_a}}, \tag{20}$$

given in [12](p.324). This continued fraction needs to be truncated and substituted into (8) to find a proper approximation for χ. Here, is chosen to truncate (20) at locations a and b, because in these special cases there are no square roots in the resulting approximation of the logarithmic temperature derivative in (8). Hence, it is more easy to derive explicit approximations for χ, V, and τ_{inv}. In the appendix the truncations at location a and b are derived for various combinations of amplitude and phase. In this section only the truncation

at location b is given using two amplitudes and one phase, i.e. $A'(\omega_1)/A(\omega_1)$, $\phi'(\omega_1)$, and $A'_2(\omega)/A(\omega_2)$, because in a numerical comparison this gave the best result. This does not necessarily mean that in practice it also gives the best result, for instance calibration errors will influence this approximation more than the one based on two phases due to the sensitivity of the amplitude to these calibration errors.

Although, it is now possible to calculate explicit solutions for χ, V, and τ_{inv}, the calculations are too complicated to do by hand. Therefore, Mathematica© was used to derive approximations for χ, V, and τ_{inv} based on the truncation in (20). This yields three solutions, however, only one is different from $\chi = 0$, which given by

$$\chi_{\Phi 4a} = \frac{3}{2}\frac{6859\rho^3\omega_1^2\phi_1' dA\left(\omega_1^2\left(dA^2+(\phi_1')^2\right)-2\omega_1\omega_2\phi_1'\phi_2'+\omega_2^2(\phi_2')^2\right)}{8\left(1311o_1^2\omega_1 dA+10108o_1\omega_1^2 dA^2+27436\omega_1^3 dA^3+45o_1^3\right)}, \tag{21}$$

where

$$dA = \frac{A_1'}{A_1}-\frac{A_2'}{A_2}, \quad o_1 = \omega_1\left(dA\left(\frac{A_1'}{A_1}\rho-4\right)+\rho(\phi_1')^2\right)-\rho\omega_2\phi_1'\phi_2'. \tag{22}$$

The corresponding V and τ_{inv} are given by

$$V_{\Phi 4a} = -\chi_{\Phi 4a}\frac{30o_l}{38\rho\omega_1 dA} \tag{23}$$

and (subscripts $\Phi 4a$ have been omitted)

$$\tau_{\Phi 4a} = \frac{3}{2}\chi\frac{-15\frac{A_1'}{A_1}\rho^2\omega\frac{1}{\chi}-24\left(\frac{V}{2\chi}\right)^2\rho^2\phi'-38\left(\frac{V}{2\chi^2}\right)\rho^2\omega+96\left(\frac{V}{2\chi}\right)\rho\phi'+60\rho\omega\frac{1}{\chi}-120\phi'}{15\rho^2\phi'}. \tag{24}$$

These solutions are complicated, but are the only explicit approximations found for the combined problem of estimating χ under convectivity and damping. The other approximations are given in the appendix. All the approximations are summarized and compared in the next section.

IV. INWARD SOLUTIONS

In this section, the different approximations to determine χ, V, and, τ_{inv} are summarized and compared for heat waves traveling towards the center. The approximations are based on the underlying models (8) and (10), which are used to calculate A'/A and ϕ' for a large number of combinations of the transport coefficients. In addition, the semi-infinite approximations derived in [1, 2] can also be used. The comparison is based on five parameters

(ρ, ω, χ, V, and τ_{inv}) and is presented in terms of normalized transport coefficients, i.e. $\bar{\chi} = \chi/\omega$, $\bar{V} = V/\omega$, and $\bar{\tau}_{inv} = \tau_{inv}/\omega$. In case two harmonics are necessary, $A'/A\,(\omega_1)$, $A'/A\,(\omega_2)$, $\phi'\,(\omega_1)$, and $\phi'\,(\omega_2)$ are calculated using $\omega_1 = \omega$ and $\omega_2 = 2\omega$ corresponding to the first and second harmonic. Note, that if it is arbitrary for the discussion to use the normalized transport coefficients $\bar{\chi}$, $\bar{V}$, and $\bar{\tau}_{inv}$ or the normal transport coefficients χ, V, and τ_{inv} the latter notation is used.

A. Overview of possible explicit approximations

In Table I all derived approximations from Section III and the appendix to estimate χ are summarized.

χ	Equation for χ	V	τ_{inv}
Approximations based on symmetry boundary condition			
χ_z	$\frac{3}{2}\frac{\omega}{\Im(z^2)}$ (see Table II for z)	0	(19)
$\chi_{Is\phi}$	$\frac{3}{4}\frac{\omega}{\phi'}\rho$	0	(14)
$\chi_{Is2\phi}$	$\frac{3}{2}\omega\rho\frac{2+\sqrt{4-\rho^2(\phi')^2}}{8\phi'}$	0	0
χ_{Is2A}	$\omega\frac{3\rho^3\sqrt{4-A'/A\rho}}{16\rho^2\sqrt{A'/A}}$	0	0
$\chi_{\Phi 2V}$	$\frac{9\rho\omega}{4\phi'(\frac{A'}{A}\rho+3)}$	(B6)	0
$\chi_{\Phi 4V}$	$\frac{3}{2}\frac{6859\rho^3\omega\phi'}{l_2+\left(6\frac{A'}{A}\rho\left(15\frac{A'}{A}\rho+32\right)+680\right)\cdot\left(2\frac{A'}{A}\rho-l_1+30\right)}$ $l_1=\sqrt{4\left(\frac{A'}{A}\rho+15\right)^2-285\rho^2(\phi')^2}$ $l_2=114\rho^2(\phi')^2\left(32\frac{A'}{A}\rho+l_1+62\right)$	(B11)	0
$\chi_{\Phi 4a}$	$\frac{3}{2}\frac{6859\rho^3\omega_1^2\phi_1' dA\, o_2}{8\left(1311o_1^2\omega_1 dA+10108o_1\omega_1^2dA^2+27436\omega_1^3dA^3+45o_1^3\right)}$ $o_1=\omega_1\left(dA\left(\frac{A_1'}{A_1}\rho-4\right)+\rho(\phi_1')^2\right)-\rho\omega_2\phi_1'\phi_2'$ $o_2=\left(\omega_1^2\left(dA^2+(\phi_1')^2\right)-2\omega_1\omega_2\phi_1'\phi_2'+\omega_2^2(\phi_2')^2\right)$	(23)	(24)
$\chi_{\Phi 4b}$	$\frac{3}{2}\frac{6859d\omega\rho^3\omega_1\phi_1'\left(\omega_2^2\left((dA)^2+\left(\phi_1'\right)^2\right)+\omega_1\phi_2'(d\omega-\omega_2\phi_1')\right)}{8(19d\omega+o)(1444d\omega^2+456d\omega o+45o^2)}$ $d\omega=\omega_1\phi_2'-\omega_2\phi_1'\; dA=\frac{A_1'}{A_1}-\frac{A_2'}{A_2}$ $o=\frac{A_1'}{A_1}\rho\omega_1\phi_2'-\frac{A_2'}{A_2}\rho\omega_2\phi_1'-4d\omega$	(B15)	(B16)
Approximations based on semi-infinite domain			
χ_c	$\frac{3}{4}\frac{\omega}{\phi'\left(\frac{A'}{A}+\frac{1}{2\rho}\right)}$ from [5]	0	see [2]
χ_ϕ	$\frac{3}{4}\sqrt{\frac{\left(\omega_1\phi'_{\omega_2}\right)^2-\left(\omega_2\phi'_{\omega_1}\right)^2}{\phi'^2_{\omega_1}\phi'^2_{\omega_2}\left(\phi'^2_{\omega_1}-\phi'^2_{\omega_2}\right)}}$	see [1]	see [1]

Table I: Overview of the approximations for χ for heat waves traveling traveling towards the center in a cylindrical geometry where a symmetry boundary condition is assumed. From left to right the columns denote: the approximation of χ either explicit or in terms of z in which case Table II gives the relationship for z; the equation numbers for χ, V and τ_{inv} refer either to Section III or to the appendix or the reference in which they are derived. The short-hand notations $\phi'(\omega_1)=\phi_1'$ and $\frac{A'(\omega_1)}{A(\omega_1)}=\frac{A_1'}{A_1}$ are used, which also means two harmonics are necessary.

Some infinite domain solutions from [1, 2] are also included in Table I. The reason is that if cylindrical effects are small, i.e. the ratio of $\omega\rho/\chi$ is large, the infinite domain approximations

give a good approximation again. However, in case z polynomials are used based on infinite domains different solutions need to be selected. The reason is that A'/A and ϕ' are negative for heat waves traveling towards the wall and are positive for heat waves traveling towards the center.

In Table I is chosen to only represent χ to keep the tables compact. The equation numbers for the corresponding V and τ_{inv} are given instead.

χ	Equation for z	Eq.
χ_{It3}	$a_3 = 2\rho^2, \quad a_2 = \left(3\rho - 2\rho^2\frac{\Theta'}{\Theta}\right)$ $a_1 = -4\rho\frac{\Theta'}{\Theta}, \quad a_0 = -6\frac{\Theta'}{\Theta}$	(A3)
$p_2 = -27a_0a_3^2 + 9a_1a_2a_3 - 2a_2^3,\ p_0 = 3a_1a_3 - a_2^2$ $p_1 = \sqrt[3]{p_2 + \sqrt{4p_0^3 + p_2^2}},\ z = \frac{1}{a_3}\left(-\frac{a_2}{3} - \frac{\sqrt[3]{2}p_0}{3p_1} + \frac{p_1}{3\sqrt[3]{2}}\right)$		
χ_{It1}	$b_2 = \rho, \quad b_1 = -\frac{\Theta'}{\Theta}\rho, \quad b_0 = -2\frac{\Theta'}{\Theta}$	(A2)
$z = \left(-b_1 + \sqrt{b_1^2 - 4\,b_0\,b_2}\right)/b_2$		
χ_{Is2}	$c_2 = \frac{\Theta'}{\Theta}\rho^2 - 4\rho, \quad c_1 = 0, \quad c_0 = 8\frac{\Theta'}{\Theta}$	(12) at a_2
χ_{Is3}	$c_2 = \rho^3, \quad c_1 = 24\rho - 8\rho^2\frac{\Theta'}{\Theta}, \quad c_0 = -48\frac{\Theta'}{\Theta}$	(12) at a_3
χ_{Is4}	$c_2 = 12\rho^3 - \frac{\Theta'}{\Theta}\rho^4, \quad c_1 = 192\rho - 72\frac{\Theta'}{\Theta}\rho^2$ $c_0 = -384\frac{\Theta'}{\Theta}$	(16)
$z^2 = \left(-c_1 + \sqrt{c_1^2 - 4\,c_0\,c_2}\right)/c_2$		

Table II: Overview of approximations for χ in terms of z for heat waves traveling towards the center in a cylindrical geometry where a symmetry boundary condition is assumed. This table denotes the coefficients to calculate z using $\Theta'/\Theta = A'/A + i\phi'$ and ρ, which is used to calculate $\chi = \frac{3}{2}\omega/\Im\left(z^2\right)$ and $\tau_{inv} = \omega\Re\left(z^2\right)/\Im\left(z^2\right)$; the equation numbers refer either to Section III or to the appendix.

In Table II the polynomials expressed in terms of z using $\Theta'/\Theta = A'/A + i\phi'$ and ρ to directly calculate χ and τ_{inv} are given. In Table III the approximations in terms of polynomials in z are given for approximations based on infinite domains.

χ_z^{inw}	Equation for z
χ_{Kc2}^{inw}	$b_2 = 4\rho, \quad b_1 = 3 + 4\frac{\Theta'}{\Theta}\rho, \quad b_0 = \frac{\Theta'}{\Theta}$
χ_{Kj2}^{inw}	$b_2 = 8\rho^2, \quad b_1 = 8\rho^2\frac{\Theta'}{\Theta} + 12\rho, \quad b_0 = 8\frac{\Theta'}{\Theta}\rho + 3$
$z = \left(-b_1 - \sqrt{b_1^2 - 4\,b_0\,b_2}\right)/b_2$	
χ_{Kj3}^{inw}	$a_3 = 16\rho^3, \quad a_2 = 16\frac{\Theta'}{\Theta}\rho^3 + 56\rho^2$ $a_1 = 48\frac{\Theta'}{\Theta}\rho^2 + 45\rho, \quad a_0 = 23\frac{\Theta'}{\Theta}\rho + 7.5$
χ_{Kc5}^{inw}	$a_3 = 16\rho^2, \quad a_2 = \left(36\rho + 16\rho^2\frac{\Theta'}{\Theta}\right)$ $a_1 = \left(15 + 28\rho\frac{\Theta'}{\Theta}\right), \quad a_0 = 3\frac{\Theta'}{\Theta}$
$p_2 = -27a_0a_3^2 + 9a_1a_2a_3 - 2a_2^3,\ p_0 = 3a_1a_3 - a_2^2$ $p_1 = \sqrt[3]{p_2 + \sqrt{4p_0^3 + p_2^2}},\ z = \frac{1}{a_3}\left(-\frac{a_2}{3} + \frac{1-i\sqrt{3}}{3\cdot\sqrt[3]{4}}\frac{p_0}{p_1} - \frac{1+i\sqrt{3}}{6\cdot\sqrt[3]{2}}p_1\right)$	

Table III: Overview of approximations for χ in terms of z for heat waves traveling towards the edge in a cylindrical geometry where an infinite domain is assumed. This table denotes the coefficients to calculate z using $\Theta'/\Theta = A'/A + i\phi'$ and ρ, which is used to calculate $\chi = \frac{3}{2}\omega/\Im\left(z^2\right)$ and $\tau_{inv} = \omega\Re\left(z^2\right)/\Im\left(z^2\right)$ resulting from $z = \sqrt{\frac{3}{2}\frac{i\omega+\tau_{inv}}{\chi}}$; the equation numbers refer either to Section III or to the appendix.

As the correct solutions switch compared to the analysis of heat waves traveling towards the wall the superscript *inw* (inward) is added. The correct solutions have been selected by comparing the three possibilities numerically. The other outward solutions given in [2] can also still be used with the only exceptions of χ_{AEK} and $\chi_{AE\Phi}$ as they approximate χ in a strong cylindrical geometry for the outward case, which is very differently for the inward case.

The approximations in Table I, Table II, and Table III are compared in the rest of this section.

B. Selection of interesting approximations

The comparison of the approximations when only the diffusivity χ is present, i.e. $V = 0$ and $\tau_{inv} = 0$, is made based on a large number of possibilities of ρ and the combined parameter $\bar{\chi} = \chi/\omega$. Therefore, (8) and (10) are used to generate A'/A and ϕ'. The most interesting and best approximations are shown in Fig. 1 in terms of the relative error with

respect to the true diffusivity χ.

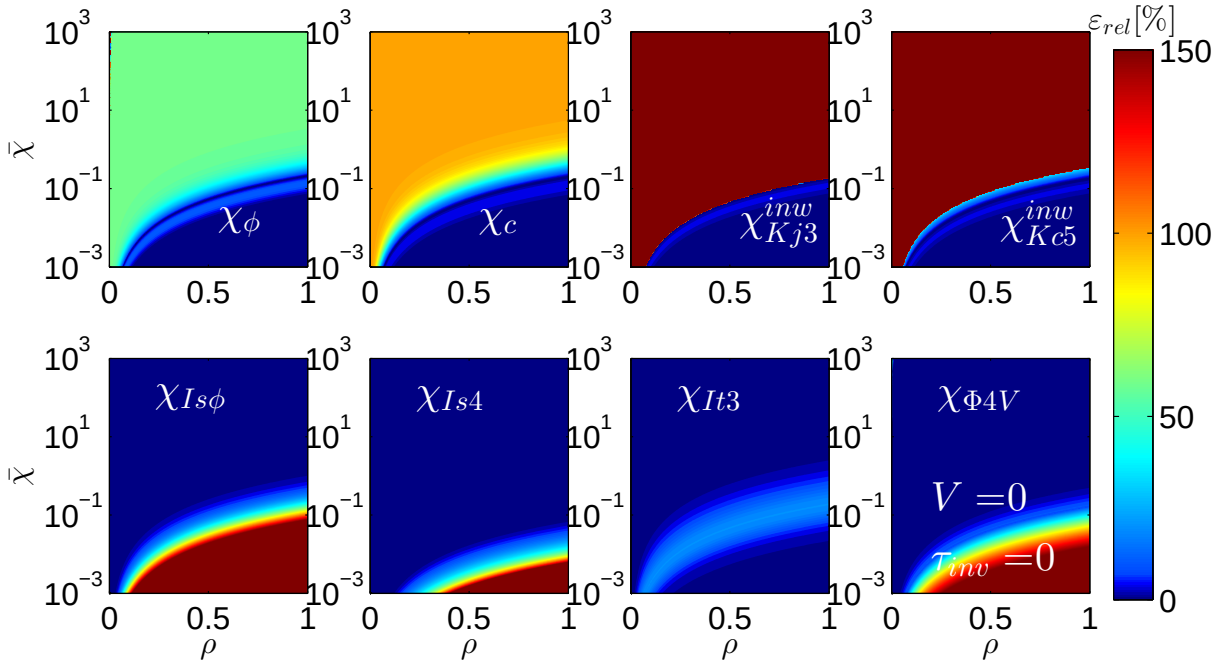

Figure 1: Comparison between the different relative errors of the χ estimates for a large range of $\bar{\chi} = \chi/\omega$ and ρ. The relative error is defined as $\varepsilon_{rel} = 100 \times \frac{|\chi - \chi_{est}|}{\chi}$ [%], where χ_{est} is either χ_ϕ from Table I, χ_c from Table I, χ^{inw}_{Kj3} Table III using (18), and χ^{inw}_{Kc5} from Table III using (18). These are the approximations based on infinite domains (first row). The true cylindrical models (second row) are estimated by either $\chi_{Is\phi}$ from (14), χ_{Is4} from (16), χ_{It3} from (A3), and $\chi_{\Phi 4V}$ from (B8). This comparison is based on a cylindrical geometry using a symmetry boundary condition with χ and $V = \tau_{inv} = 0$, where the heat waves travel inwards. The darkest blue represents $\varepsilon_{rel} < 1\%$ and the darkest red represents all $\varepsilon_{rel} > 150\%$.

The use of infinite domain approximations for heat waves traveling to the center give a good approximation if the ratio $\rho\omega/\chi$ is large. In that case χ_c has the largest region with a good accuracy, but the highest accuracy is generally given by χ_{Kj3}. In that case the approximations based on cylindrical geometry for heat waves traveling towards the center give good approximations for χ. Hence, χ_{It3} almost approximates the entire presented region well be it with a slightly less accuracy then χ_{Is4}. Also $\chi_{\Phi 4V}$ performs well, but it is mainly derived to perform well under convectivity. $\chi_{Is\phi}$ is also shown as it is the most simple cylindrical approximation found. Unfortunately, its region of applicability is much smaller than the other approximations.

In summary, χ_{It3} has the largest region of applicability. Only in a small region its relative error is larger (maximally $\varepsilon_{rel} \approx 30\%$). In this region different approximations are necessary, for instance χ_{Kj3} or χ_c and χ_{Is4}.

C. Diffusivity and damping only

It is not possible to use one approximation to approximate χ well for all combinations of χ, ω, ρ, and τ_{inv}. However, it turns out that by combining two approximations to estimate χ almost the entire presented region of interest for heat waves traveling inwards can be covered. This is shown in Fig. 2, where the maximum error over the entire presented region is $\varepsilon_{rel} < 2\%$ such that it is always possible to get an accurate result for the presented combination of χ, ω, τ_{inv} and ρ.

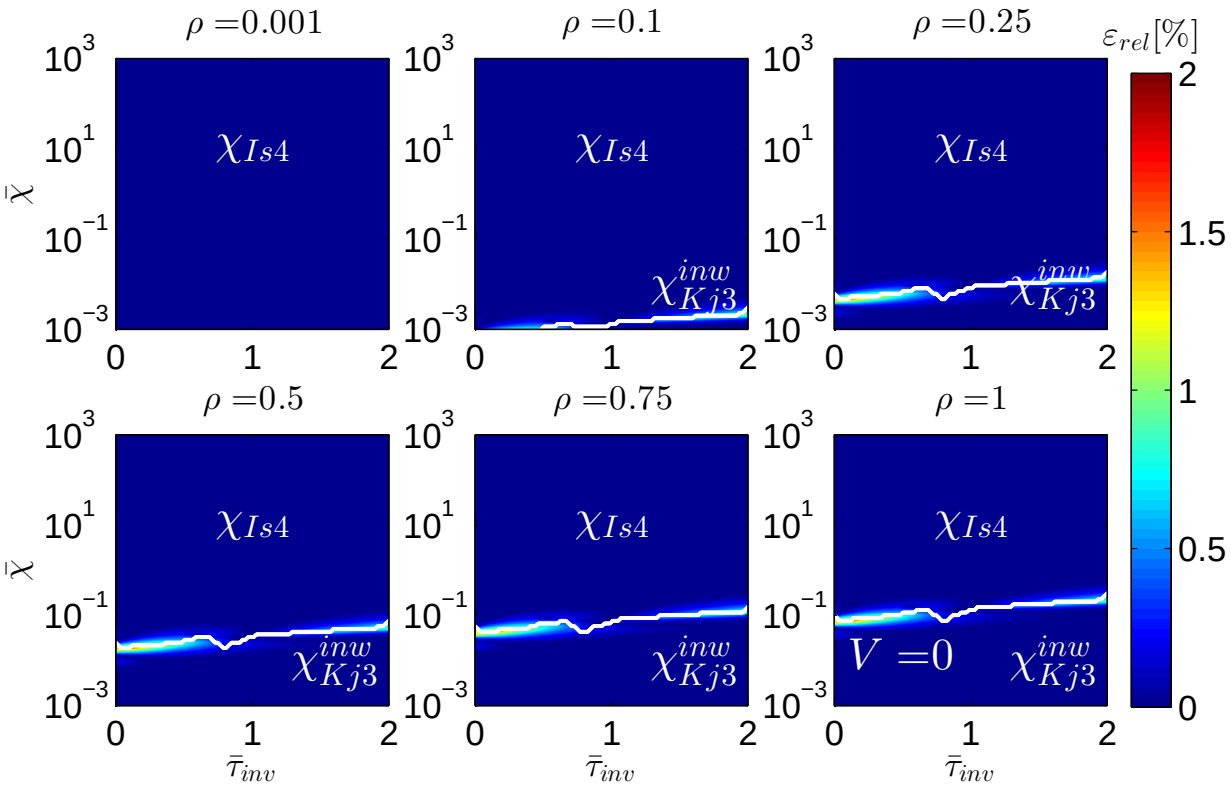

Figure 2: Relative error of the χ estimates for the combination of χ_{Is4} and χ^{inw}_{Kj3} presented for different $\bar{\chi} = \chi/\omega$ and $\bar{\tau}_{inv} = \tau_{inv}/\omega$ represented at a number of spatial locations ρ. The relative error is defined as $\varepsilon_{rel} = 100 \times \frac{|\chi - \chi_{est}|}{\chi}$ [%]. This figure combines the approximations χ_{Is4} and χ^{inw}_{Kj3}, which are separated by the boundary represented by the white line. This figure is based on a cylindrical geometry using a symmetry boundary condition with $V = 0$, where the heat waves travel inwards.

Both, χ^{inw}_{Kj3} and χ_{Is4} have been chosen, because they give the most accurate approximations in their regions of applicability and they are complementary. The white line shows the approximate boundary of the regions of applicability of χ^{inw}_{Kj3} and χ_{Is4}. At this boundary the error is largest.

D. Diffusivity and convectivity with $\tau_{inv} = 0$ and $\tau_{inv} = 2$

For the inward case multiple approximations are available to estimate V. It is not easy to choose a suitable approximation before the measurements have been analyzed, because the approximations all depend on different harmonic information. For instance, χ_{ϕ} uses only the

phases of two harmonics, but $\chi_{\Phi 4a}$ uses two phases and one amplitude point. On the other hand, when $\tau_{inv} = 0$, then $\chi_{\Phi 4V}$ can be used, which uses only one harmonic. Therefore, it is not possible to point out a best approximation. However, the regions of applicability of the approximation are again clearly defined. χ_ϕ which originates from slab-geometry is best at approximating χ for large $\omega\rho/\chi$. On the other hand, the approximations based on the symmetry boundary conditions estimate χ well for small $\omega\rho/\chi$.

From a numerical point of view $\chi_{\Phi 4Va}$ performed best, but it is comparable to the other cylindrical approximations. Therefore, it is chosen to combine $\chi_{\Phi 4Va}$ and χ_ϕ separated by the white line, which is shown in Fig. 3 and Fig. 4 for $\tau_{inv} = 0$ and $\tau_{inv} = 2$.

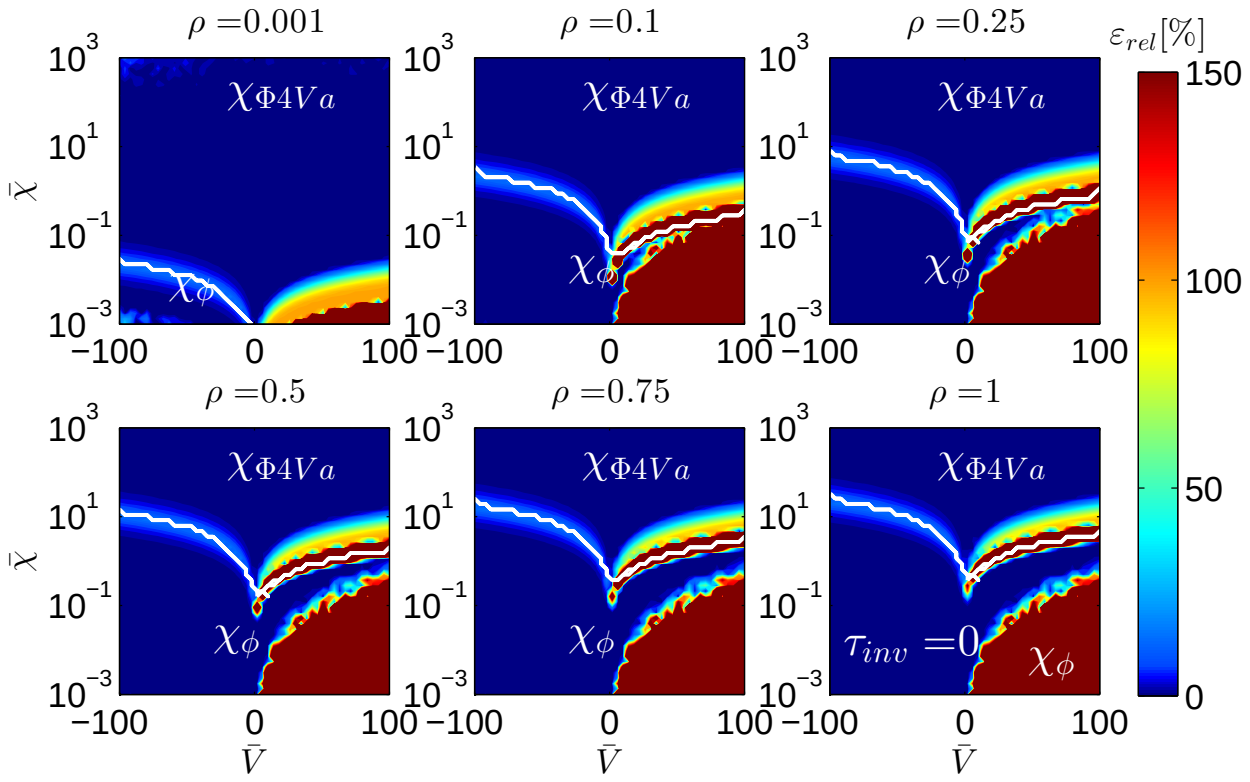

Figure 3: Relative error of the χ estimates for the combination of $\chi_{\Phi 4Va}$ and χ_ϕ presented for different $\bar{\chi} = \chi/\omega$ and $\bar{V} = V/\omega$ represented at a number of spatial locations ρ. The relative error is defined as $\varepsilon_{rel} = 100 \times \frac{|\chi - \chi_{est}|}{\chi}$ [%]. This figure combines the approximations $\chi_{\Phi 4Va}$ and χ_ϕ, which are separated by the boundary represented by the white line. This figure is based on a cylindrical geometry using a symmetry boundary condition with $\tau_{inv} = 0$, where the heat waves travel inwards. The darkest blue represents $\varepsilon_{rel} < 1\%$ and the darkest red represents all $\varepsilon_{rel} > 150\%$.

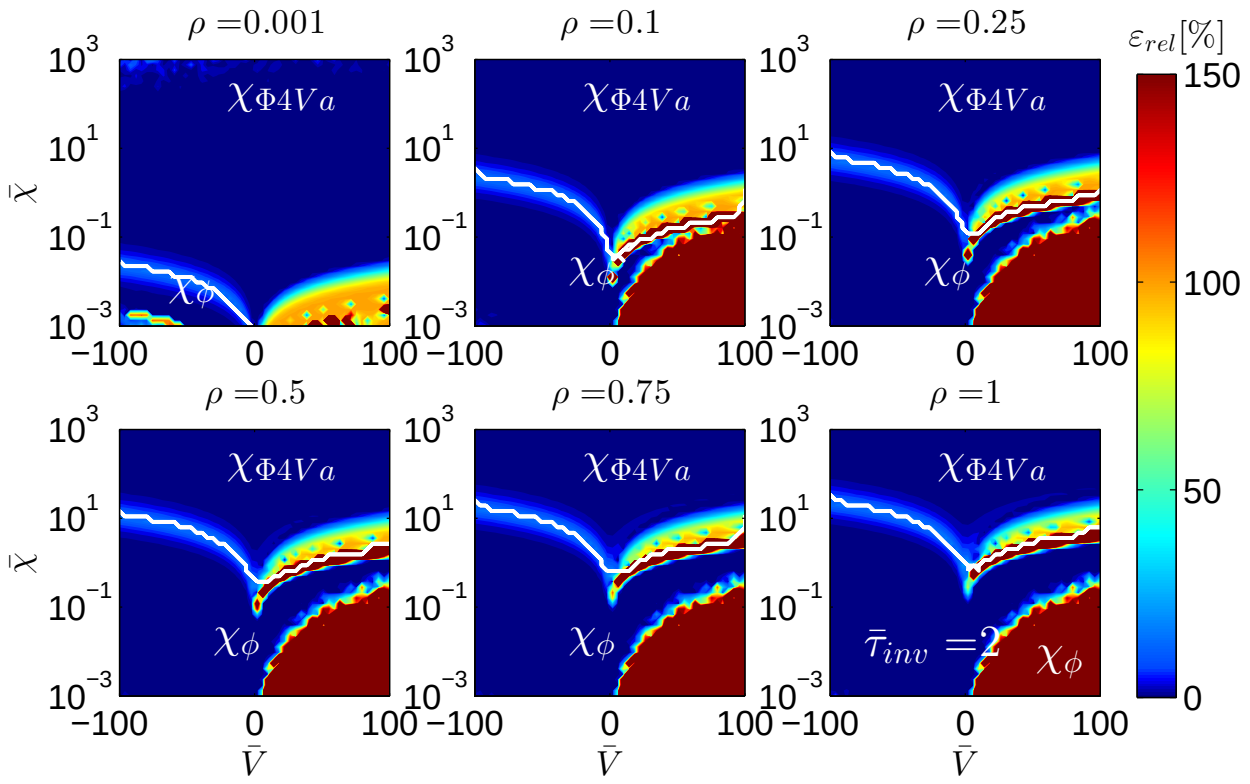

Figure 4: Relative error of the χ estimates for the combination of $\chi_{\Phi 4Va}$ and χ_ϕ presented for different $\bar{\chi} = \chi/\omega$ and $\bar{V} = V/\omega$ represented at a number of spatial locations ρ. The relative error is defined as $\varepsilon_{rel} = 100 \times \frac{|\chi - \chi_{est}|}{\chi}$ [%]. This figure combines the approximations $\chi_{\Phi 4Va}$ and χ_ϕ, which are separated by the boundary represented by the white line. This figure is based on a cylindrical geometry using an symmetry boundary condition with $\bar{\tau}_{inv} = 2$, where the heat waves travel inwards. The darkest blue represents $\varepsilon_{rel} < 1\%$ and the darkest red represents all $\varepsilon_{rel} > 150\%$.

Both figures show similar regions where χ can be estimated well and where not. The large error close to the boundary is caused by the limited region of approximation, which is similar to the previous figures. There is no suitable approximation, which handles the regions with large errors.

V. SUMMARY AND DISCUSSION

In this paper, the problem of determining the thermal diffusion coefficient from electron temperature measurements during power modulation experiments has been revisited. A large number of new approximations have been introduced to estimate χ directly from A'/A

and ϕ' for different combinations of χ, V, and τ_{inv} for heat waves traveling to the center. This corresponds to the case of off-axis heating. The approximations are based on a symmetry boundary conditions and are derived on the basis of cylindrical geometry using common assumptions.

The quality of the approximations is presented in several figures. In case only χ and τ_{inv} are considered ($V = 0$), the relative error of the χ estimate for the region of interest are $\varepsilon_{rel} < 2\%$. These errors are achievable by combining χ^{inw}_{Kj3} and χ_{Is4}. In case also V is considered the new approximations show a significant region in which χ can be estimated well, but also regions in which no suitable approximation exists. Combining $\chi_{\Phi 4Va}$ and χ_{ϕ} cover a large region where χ can be well estimated.

VI. GENERAL CONCLUSION

In this set of papers (Part 1, Part 2, and Part 3), the problem of determining the thermal diffusion coefficient from electron temperature measurements during power modulation experiments has been revisited. A large number of new approximations have been introduced to estimate χ directly from A'/A and ϕ' for different combinations of χ, V, and τ_{inv}. The approximations are based on infinite domains or Neumann boundary conditions and are derived on the basis of slab or cylindrical geometry using common assumptions. These approximations including the well known approximations from the literature have been compared in Part 3 for heat waves traveling towards the center (inward) and Part 1 and Part 2 towards the edge (outwards). The approximations are derived based on A'/A and ϕ'. The quality of the approximations is presented in several figures. In case only χ and τ_{inv} are considered ($V = 0$), the relative error of the χ estimate for the region of interest is in general $\varepsilon_{rel} < 1\%$. However, in a small region the errors are larger with a maximum relative error for heat waves traveling towards the edge $\varepsilon_{rel} < 20\%$ and for heat waves traveling towards the center $\varepsilon_{rel} < 2\%$. These errors are achievable by combining χ_{Kj3} and $\chi_{AE\Psi}$ in the outward case χ^{inw}_{Kj3} and χ_{Is4} in the inward case respectively. In case also V is considered the new approximations show a significant region in which χ can be estimated well, but also regions in which no suitable approximation exists. Combining $\chi_{\Phi 4Va}$ and χ_{ϕ} for the inward case and $\chi_{AE\Psi}$ and χ_{ϕ} for the outward case cover a large region where χ can be well estimated

However, there are also a number of important issues when using the approximations

presented in these parts and the literature. First of all, the combination of assuming the transport coefficients independent of ρ and the use of infinite domains or symmetry boundary conditions necessary to arrive at explicit approximations can result in errors. These errors are introduced as in reality the profiles may vary spatially and different boundary conditions are present. In Part 1, it has been shown that these errors influence the estimation of the convectivity and the damping more significantly making the estimated V and τ_{inv} often erroneous. On the other hand, as has been shown in Part 2, it is important to still estimate V and τ_{inv} as they are necessary to select the proper approximation and to arrive at correct estimates of χ in the presence of V and τ_{inv}. A second important issue is the determination of A'/A and ϕ' from ϕ and A. To investigate this relationship the notion of transfer functions has been introduced, which makes the relationship between A'/A and A, and, ϕ' and ϕ explicit. It showed that the relationship in slab-geometry is straightforward (Part 1), but in cylindrical geometry is complicated (Part 2). It also shows that the dependency of ρ is contained in A' and ϕ' and as such depend on how A' and ϕ' are calculated. Therefore, it is always important to clearly state how A' and ϕ' are calculated from ϕ and A to arrive at comparable results. However, for cylindrical domains there is not a clear recipe to calculate A' and ϕ' from ϕ and A. Hence, in this paper we refrain on commenting on that and for the analysis the true A'/A and ϕ' are used. A third problem, only touched upon briefly, is the effect of noise, which is not taken into account by the methods proposed in this set of papers. However, if two harmonics are used (in the presence of V), it is important that both harmonics do not contain to much noise, which can be achieved by using a non-symmetric duty cycle.

These issues are partly related to the use of explicit approximations. These problems can in principle be avoided by using implicit methods. As these implicit methods allow the use of a more realistic boundary conditions, the direct estimation of χ from A and ϕ using the transfer function representation, and the inclusion of noise in the estimation processes. However, such implicit methods will come at the price of more complex optimization problems and require a number of different concepts as presented in this set of papers. Nevertheless, in case implicit methods are used finding good starting values is also important for which the approximations presented in this set of papers can be used.

VII. ACKNOWLEDGMENTS

The first author is an international research fellow of the Japan Society for the Promotion of Science and hence wishes to express his gratitude to the JSPS for making this research possible. This project has received funding from the European Union's Horizon 2020 research and innovation programme under grant agreement number 633053. The views and opinions expressed herein do not necessarily reflect those of the European Commission. This work is also supported by NWO-RFBR Centre-of-Excellence on Fusion Physics and Technology (Grant nr. 047.018.002).

APPENDIX

The appendix consists of three sections in which approximations are derived based on the continued T-fraction of modified Bessel functions of the first kind to arrive at approximations for χ and τ_{inv} in terms of z. In addition, the other approximations for χ, V, and τ_{inv} based on the continued fraction given in (20) are presented. Finally, also an approximation is given for a case where only χ is present.

Appendix A: CONTINUED T-FRACTION OF THE RATIO OF BESSEL FUNCTIONS OF THE FIRST KIND

The following continued T-fraction of $I_2(z\rho)/I_1(z\rho)$ is based on [12](p. 363) and is useful for approximating (10). The continued T-fraction is given by

$$\frac{I_2(z\rho)}{I_1(z\rho)} = \cfrac{z\rho}{2 + z\rho\big|_a + \cfrac{-3z\rho}{3 + 2z\rho\big|_b + \cfrac{-5z\rho}{4 + 2z\rho + \cdots}}}. \tag{A1}$$

This continued fraction is truncated at locations a and b.

a) Truncating (A1) at location a results in polynomial

$$0 = \rho z^2 - \frac{\Theta'}{\Theta}\rho z - 2\frac{\Theta'}{\Theta}. \tag{A2}$$

b) Truncating (A1) at location b results in third order polynomial

$$0 = 2\rho^2 z^3 + \left(3\rho - 2\rho^2 \frac{\Theta'}{\Theta}\right) z^2 - 4\rho \frac{\Theta'}{\Theta} z - 6\frac{\Theta'}{\Theta}. \tag{A3}$$

Again, continued fractions with more terms result in 4th order or higher polynomials.

Appendix B: CONTINUED C-FRACTION OF CONFLUENT HYPERGEOMETRIC FUNCTION OF THE FIRST KIND

The continued C-fraction for $\Phi(a+1, b+1, z)/\Phi(a, b, z)$ given in (20) is used to derive several approximations.

a) Truncating (20) at location a and substituting it into (8) results in following logarithmic temperature derivative

$$\frac{\Theta'}{\Theta} = \lambda_1 + \lambda_2 \frac{1}{1 - \dfrac{\dfrac{\lambda_2 - \lambda_1 - \lambda_2}{2}\rho}{1 + \dfrac{\lambda_2 + (\lambda_2 - \lambda_1)}{6}\rho}}. \tag{B1}$$

This can be further simplified by partly substituting λ_1 and λ_2

$$\frac{\Theta'}{\Theta} = \frac{2\lambda_1^2\rho + \lambda_1\lambda_2\rho + 2\lambda_2^2\rho - 6\frac{V}{\chi}}{6 - 2\frac{V}{\chi}\rho}, \tag{B2}$$

where $2\lambda_1^2 + \lambda_1\lambda_2 + 2\lambda_2^2 = 2\left(\frac{V}{\chi}\right)^2 + \frac{9}{2}\frac{\tau_{inv}+\omega i}{\chi}$ such that

$$\left(6 - 2\frac{V}{\chi}\rho\right)\frac{A'}{A} + \left(6 - 2\frac{V}{\chi}\rho\right) i\phi' = \left(2\left(\frac{V}{\chi}\right)^2 + \frac{9}{2}\frac{\tau_{inv} + \omega i}{\chi}\right)\rho - 6\frac{V}{\chi}. \tag{B3}$$

By splitting (B3) in its real and imaginary part χ can be calculated

$$\left(6 - 2\frac{V}{\chi}\rho\right)\phi' = \frac{9}{2}\frac{\omega}{\chi}\rho \tag{B4}$$

and

$$\left(6 - 2\frac{V}{\chi}\rho\right)\frac{A'}{A} = 2\left(\frac{V}{\chi}\right)^2\rho + \frac{9}{2}\frac{\tau_{inv}}{\chi}\rho - 6\frac{V}{\chi}. \tag{B5}$$

The imaginary part for $V = 0$ yields an approximation for χ, i.e.

$$\chi_{Is\phi} = \frac{3}{4}\frac{\omega}{\phi'}\rho \qquad \text{and} \qquad \tau_{Is\phi} = \frac{\omega}{\phi'}\frac{A'}{A}, \tag{14}$$

which is also found using asymptotic expansions and in (14) using a continued fraction based on Bessel functions. If τ_{inv} is assumed to be zero, solve (B4) and (B5) together

$$\chi_{\Phi 2V} = \frac{9\rho\omega}{4\phi'(\frac{A'}{A}\rho + 3)} \qquad \text{and} \qquad V_{\Phi 2V} = -\frac{9\frac{A'}{A}\rho\omega}{4\phi'(\frac{A'}{A}\rho + 3)}. \tag{B6}$$

The mixed case of χ, V, and τ_{inv} cannot be solved, due to the system of equations even if one harmonic is added.

b) Truncating (20) at location b and substituting it into (8) results in following logarithmic temperature derivative by substituting λ_1 and λ_2

$$\frac{\Theta'}{\Theta} = -\frac{\rho^2 V\left(6V^2 + 19\chi(\tau_{inv} + i\omega)\right) - 12\rho\chi\left(4V^2 + 5\chi(\tau_{inv} + i\omega)\right) + 120V\chi^2}{3\chi\left(\rho^2\left(2V^2 + 5\chi(\tau_{inv} + i\omega)\right) - 16\rho V\chi + 40\chi^2\right)}. \tag{B7}$$

The complexity of (B7) makes it difficult to calculate approximations by hand. Therefore, Mathematica© has been used to calculate the approximations for χ, V, and τ_{inv}.

b1) If $\tau_{inv} = 0$, (B7) results in

$$\chi_{\Phi 4V} = \frac{3}{2}\frac{6859\rho^3\omega\phi'}{l_2 - \left(6\frac{A'}{A}\rho\left(15\frac{A'}{A}\rho + 32\right) + 680\right)\cdot\left(-2\frac{A'}{A}\rho \pm l_1 + 30\right)}, \tag{B8}$$

with

$$l_1 = \sqrt{4\left(\frac{A'}{A}\rho + 15\right)^2 - 285\rho^2\left(\phi'\right)^2} \tag{B9}$$

and

$$l_2 = 114\rho^2\left(\phi'\right)^2\left(32\frac{A'}{A}\rho \pm l_1 + 62\right). \tag{B10}$$

There are two solutions possible, the second option ($-$ in $\pm$) gives a solution in a region with poor approximations and is disregarded. Hence, $+$ solution is used. The convectivity V is given by

$$V_{\Phi 4V} = \chi_{\Phi 4V}\frac{-l_1 - 17\frac{A'}{A}\rho + 30}{19\rho}. \tag{B11}$$

b2) See (21)

b3) If A_1'/A_1, ϕ_1' and ϕ_2' are used, only one solution is found

$$\chi_{\Phi 4b} = \frac{3}{2}\frac{6859d\omega\rho^3\omega_1\phi_1'\left(\omega_2^2\left((dA)^2 + (\phi_1')^2\right) + \omega_1\phi_2'(d\omega - \omega_2\phi_1')\right)}{8(19d\omega + o)\left(1444d\omega^2 + 456d\omega o + 45o^2\right)}, \tag{B12}$$

with

$$d\omega = \omega_1\phi_2' - \omega_2\phi_1' \tag{B13}$$

and

$$o = \frac{A_1'}{A_1}\rho\omega_1\phi_2' - \frac{A_2'}{A_2}\rho\omega_2\phi_1' - 4d\omega. \tag{B14}$$

The corresponding V and τ_{inv} are given by

$$V_{\Phi 4b} = -\chi_{\Phi 4b}\frac{30o}{38\rho d\omega}, \tag{B15}$$

and (subscripts $\Psi 4b$ have been omitted)

$$\tau_{\Phi 4b} = \frac{3}{2}\chi\frac{-15\frac{A_1'}{A_1}\rho^2\omega\frac{1}{\chi} - 24\left(\frac{V}{2\chi}\right)^2\rho^2\phi' - 38\left(\frac{V}{2\chi^2}\right)\rho^2\omega + 96\left(\frac{V}{2\chi}\right)\rho\phi' + 60\rho\omega\frac{1}{\chi} - 120\phi'}{15\rho^2\phi'}. \tag{B16}$$

This equation is exactly the same as (24).

Also a T-fraction is given in [11, 12], but it showed less accurate results than the continued C-fraction.

Appendix C: APPROXIMATIONS FOR χ ONLY ($V = \tau_{inv} = 0$)

If $\tau_{inv} = 0$ and $V = 0$, the truncation of (12) at a_2 is given by

$$0 = \left(\left(\frac{A'}{A} + i\phi'\right)\rho^2 - 4\rho\right)\frac{3}{2}\frac{\omega i}{\chi} + 8\left(\frac{A'}{A} + i\phi'\right). \tag{C1}$$

The real part is given by

$$0 = -\phi'\rho^2\frac{3}{2}\frac{\omega}{\chi} + 8\frac{A'}{A} \tag{C2}$$

and the imaginary part is given by

$$0 = \frac{A'}{A}\rho^2\frac{3}{2}\frac{\omega i}{\chi} - 4\rho\frac{3}{2}\frac{\omega i}{\chi} + 8i\phi'. \tag{C3}$$

Solving for A'/A and ϕ' and rewriting in terms of χ yields

$$\chi_{Is2A} = \omega\frac{3\rho^3\sqrt{4 - A'/A\rho}}{16\rho^2\sqrt{A'/A}} \tag{C4}$$

and

$$\chi_{Is2\phi} = 3\omega\rho\frac{2 + \sqrt{4 - \rho^2\left(\phi'\right)^2}}{16\phi'}. \tag{C5}$$

[1] M. van Berkel *et al.*, "Explicit approximations to estimate the perturbative diffusivity in the presence of convectivity and damping (part a): slab-geometry approximations," *submitted to Physics of Plasmas*, vol. -, pp. –, 2014.

[2] ——, "Explicit approximations to estimate the perturbative diffusivity in the presence of convectivity and damping (part b): outward approximations," *submitted to Physics of Plasmas*, vol. -, pp. –, 2014.

[3] N. J. Lopes Cardozo, "Perturbative transport studies in fusion plasmas," *Plasma Phys. Control. Fusion*, vol. 37, p. 799, 1995.

[4] S. P. Eury, E. Harauchamps, X. Zou, and G. Giruzzi, "Exact solutions of the diffusion-convection equation in cylindrical geometry," *Physics of Plasmas*, vol. 12, p. 102511, 2005.

[5] A. Jacchia, P. Mantica, F. De Luca, and G. Gorini, "Determination of diffusive and nondiffusive transport in modulation experiments in plasmas," *Physics of Fluids B*, vol. 3, no. 11, pp. 3033–3040, 1991.

[6] H. Bateman and A. Erdelyi, *Higher transcendental functions*, A. Erdelyi, Ed. Mcgraw-Hill, New York, 1953.

[7] L. Slater, *Confluent hypergeometric functions*. Cambridge University Press, Cambridge, 1960.

[8] Y. L. Luke, *The special functions and their approximations, Volume 1*, Stegun, Ed. Elsevier, 1969.

[9] A. D. Polyanin and V. F. Zaitsev, *Handbook of Exact Solutions for Ordinary Differential Equations*. Chapman & Hall/CRC, London, 2003, vol. 2.

[10] H. S. Carslaw and J. C. Jaeger, *Conduction of heat in solids*. Clarendon Press, Oxford, 1959, vol. 1.

[11] W. B. Jones and W. T. C. Fractions, *Analytic Theory and Applications*, ser. Encyclopedia of Mathematics and its Applications. Addison-Wesley Publishing Company, London, 1980, vol. 11.

[12] A. Cuyt, V. B. Petersen, B. Verdonk, H. Waadeland, and W. B. Jones, *Handbook of continued fractions for special functions*. Springer, 2008.

[13] M. Abramowitz and I. Stegun, *Handbook of mathematical functions: with formulas, graphs, and mathematical tables*. Dover, New York, 1976.